

Modelling the *Tracy* storm surge – implications for storm structure and intensity estimation

Bruce A. Harper

Systems Engineering Australia Pty Ltd

(Manuscript received October 2009, revised July 2010)

The results of hydrodynamic storm surge modelling are used to inform and construct a detailed quantitative description of the possible changing structure and intensity of severe tropical cyclone *Tracy* as it proceeded across Beagle Gulf to landfall at the City of Darwin in 1974. The measured storm surge is used as an independent wind calibration proxy to augment the measured eyewall winds and pressures from the airport, which is located close to the coast. The investigation resulted in a seemingly subtle change in the modelled wind speed for the airport site but enabled an accurate reproduction of the magnitude of the measured storm surge in the nearby harbour and wave impacts on the local beaches. It is therefore hypothesised that *Tracy* likely underwent an eyewall-replacement contraction when approaching near land west of Darwin and, locally at least, significantly increased its peak winds during the critical period when the storm tide was generated and enabled the propagation of the surge into the harbour. It is further hypothesised that the storm subsequently rapidly decayed or became unstable as it came ashore. As a result of these experiments, there is also evidence that winds at the nearby coastline may have been substantially higher than those recorded at the airport.

Introduction

In addition to the extensive devastation to housing caused by the extreme winds of *Tracy* at Darwin in December 1974, a storm surge of 1.55 m above expected tide level was also measured at the harbour tide gauge. The associated breaking wave setup and wave runup combined with the high tide of the day to create localised inundation along the coastline from Fannie Bay to Casuarina Beach, extending to an absolute height of about 5 m above Mean Sea Level (MSL). Darwin has a relatively high tide range of 8 m and fortuitously the event occurred during a neap tidal period, otherwise the impacts may have been more severe. Notwithstanding this, many vessels in Darwin Harbour were beached or sunk, including a naval patrol boat, and 22 of the 71 lives lost were at sea.

Since the late 1970s there have been several studies that examined the *Tracy* storm surge event and each has reported some degree of difficulty in matching the measured surge level within the harbour and had to adopt different assumptions and techniques to generate a suitably high response. These difficulties persist even though the

nearby Dines anemometer record at the airport is able to be adequately modelled at or near the measured peak winds by a suitably configured 'Holland' (Holland 1980; Harper and Holland 1999) parametric model. However, quantitative wind measurements elsewhere in the area are sparse compared with the extremely small scale of *Tracy* and the satellite imagery of the day is poor. Radar remains the principal reconstruction tool.

Extensive trial and error testing combined with a speculative reconstruction of the wind and pressure structure of *Tracy* was undertaken to obtain a set of wind model parameters capable of satisfying the observations of both winds and storm surge. Although the resulting wind model is simplistic, it supports other eyewitness reports of the shrinking wind swath across the city and leads to evidence that the northern suburbs likely experienced higher winds than were recorded at the airport – a conclusion also resulting from the extensive damage investigations at the time (e.g. Walker 1975).

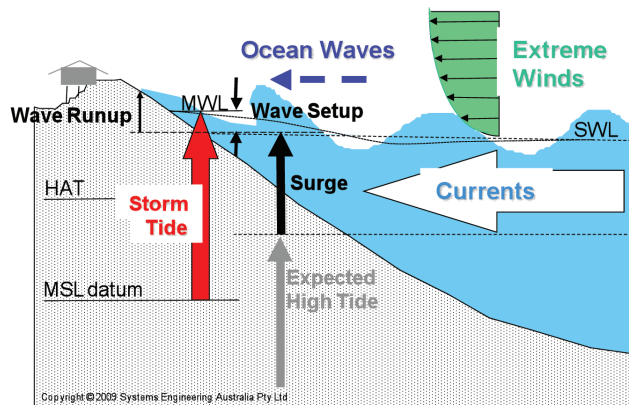
The work described here was undertaken as part of the development of the Darwin Tropical Cyclone Warning Centre (TCWC) Northern Region Storm Tide Prediction System, described in SEA (2005). The hindcasting of the effects of tropical cyclone *Tracy* was done as part of the validation of the numerical modelling systems.

Corresponding author address: Bruce A. Harper, Director
Systems Engineering Australia Pty Ltd, 106/71 Beeston St, Newstead,
Queensland 4006, Australia

Components of a storm tide

The following section provides a brief overview of the tropical cyclone storm tide phenomenon and provides some important definitions. A more detailed description is available in Harper (2001). The total seawater level experienced at a coastal, ocean or estuarine site during the passage of a severe tropical cyclone will be made up of relative contributions from a number of different effects, as depicted in Fig. 1. The combined or total water level is then termed the *storm tide*, which is an absolute vertical level, referenced to *Australian Height Datum* (AHD). Potential inundation depths at any site can then be estimated if the local ground level to AHD is also known.

Fig. 1 Water level components of an extreme storm tide.



It is important to understand the different water level components that comprise the total storm tide, namely:

(a) The astronomical tide

This is the regular periodic variation in water levels due to the gravitational effects of the Moon and Sun, which can be predicted with generally very high accuracy at any point in time (past and present) if sufficient measurements are available. The highest expected tide level at any location is termed Highest Astronomical Tide (HAT) and occurs once each 18.6 year period, although at some sites tide levels similar to HAT may occur several times per year. The tidal variation at Darwin is quite large, with a tidal range of 8.1 m and an HAT of 4.0 m AHD.

(b) Storm surge

This is the combined result of the severe atmospheric pressure gradients and wind shear stress of the cyclone acting on the underlying ocean. The storm surge is a long period 'wave' capable of sustaining above-normal water

levels over a number of hours. The wave travels with and ahead of the storm and may be amplified as it progresses into shallow waters or is confined by coastal features. Typically the length of coastline which is severely affected by a tropical cyclone storm surge is of order 100 km either side of the track although some influences may extend many hundreds of kilometres. The magnitude of the surge is affected by many factors such as storm intensity, size, speed and angle of approach to the coast and the coastal bathymetry.

(c) Breaking wave setup

Severe wind fields also create abnormally high sea conditions and extreme waves may propagate large distances from the centre of a storm as ocean swell. These waves experience little or no attenuation in deepwater regions and an offshore storm can impact several hundred kilometres of coastline. As the waves enter shallower waters they refract and steepen under the action of shoaling until their stored energy is dissipated by wave breaking either offshore or at a beach or reef. After breaking, a portion of the wave kinetic energy is converted into potential energy which, through the continuous action of many waves, is capable of sustaining shoreward water levels which are above the still-water level further offshore. This increase in still-water level after wave breaking is known as *breaking wave setup* and applies to most natural beaches and reefs. It does not apply in conditions where waves do not break incipiently but rather are degraded more gradually through frictional or diffractive effects. For example, wave setup is expected to be minimal through deepwater river entrances or where waves progress into swamps or inundated lands. Tide gauges, due to their deliberate placement, types of sensors and methods of analysis will typically not measure wave setup.

(d) Wave runup and other effects

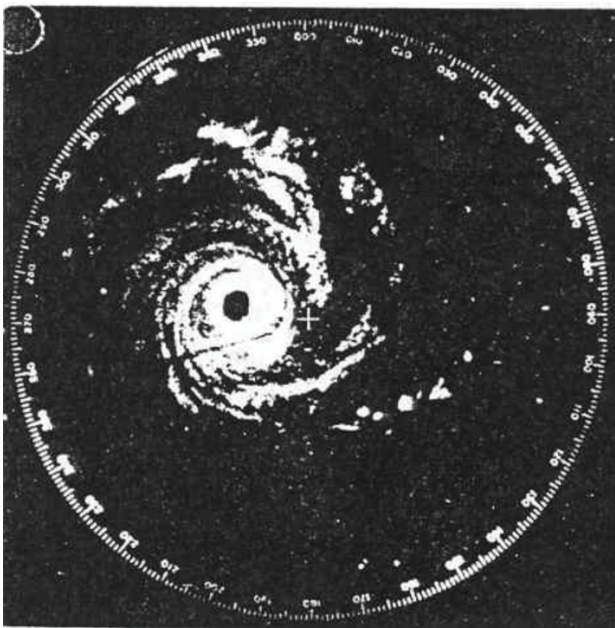
While much of the wave energy at the coast might be converted into breaking wave setup, there remains some residual energy in the form of individual waves that will generate intermittent *wave runup* and may cause localised impacts and erosion at elevations above that of the nominated storm tide level. These effects are typically localised and can only be estimated with specific information about the land-sea interface, which may be changing in time as the storm tide increases in height. This would include the slope of the shoreline, the porosity, vegetation and the incident wave height and period. There remain other related phenomena which can also affect the local water level. These may include long period shelf waves, unsteady surf beat, stormwater and/or river runoff etc.

Background to the event

Cyclone *Tracy* is perhaps the best known of all Australian tropical cyclones. Its impact at Darwin on Christmas Day 1974

resulted in massive destruction of housing in the northern suburbs around the airport and lead to the nation's largest civilian evacuation effort to enable rebuilding of the city (Cole 1977). The present investigation concentrates only on the meteorological aspects of the storm and its coastal impacts, principally as summarised in Bureau of Meteorology (1977). For example, a radar view of this extremely small cyclone is shown in Fig. 2 when the storm was close to Charles Point, about 25 km west of Darwin. The radar viewing range scale is 60 nautical miles at this time.

Fig. 2 Radar image of *Tracy* at 1445 UTC 24 December 1974.



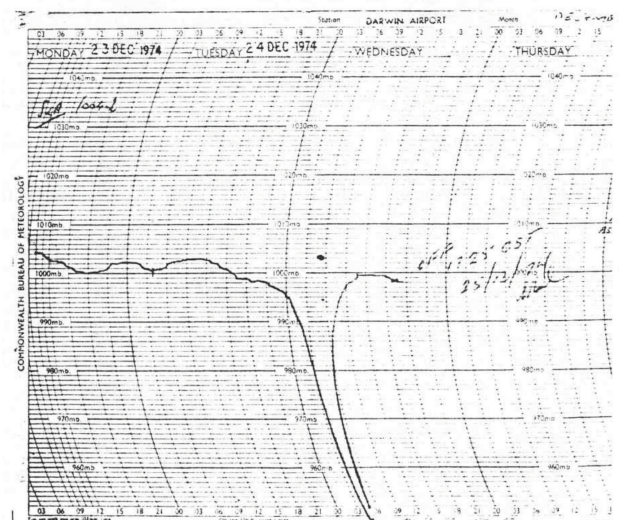
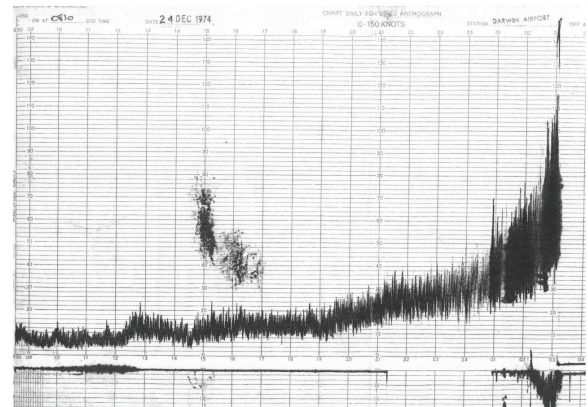
Tracy formed north of Melville Island during 22 December 1974 and moved southwest for about two days before suddenly recurving around Bathurst Island under the influence of an upper level anticyclone and heading southeast towards the Cox Peninsula, west of Darwin. By midnight on the 24 December, the centre was near Charles Point and, clearly influenced by the coast, altered course to be more nearly eastward as it slowly passed almost directly over the radar at Darwin airport at 0400 CST (1830 UTC).

Given the very high level of destruction created by *Tracy* and the fact that the anemometer was destroyed by flying debris just before the eye passed over the instrument, there will always remain some doubt as to the best estimate of the peak wind speed for this event (Harper 2002). However, there is agreement that the adjusted MSL central pressure in the eye over the airport was 950 hPa, with an ambient of 1004 hPa, and that the eye diameter was about 12 km.

The airport Dines anemometer was well located in flat open terrain about 3 km from the coast and within 500 m of the assessed storm track radar centreline. The pressure readings were also verified by comparison with mercury barometers at the nearby Weather Service Office (WSO) and

also the Regional Office, which at that time was located in the city centre about 6 km SW of the airport. Fig. 3 presents the anemograph and barograph records from the airport site.

Fig. 3 Wind and pressure record from Darwin Airport.



The airport Dines anemometer, nominally rated to 67 ms^{-1} , failed 40 minutes prior to the full calm being experienced at the site but only ten minutes prior to the passage of the Bureau of Meteorology-assessed period of maximum winds based on observer logs. The highest wind gust recording deemed reliable was 60.3 ms^{-1} , which occurred five minutes before total loss. The radar evidence suggested that the band of maximum winds had passed the site within five minutes after the failure or ten minutes after the highest reliable reading. During this time the storm forward speed was around 1.7 ms^{-1} , indicating a radial travel over ten minutes of only about 1 km. Also, detailed analysis of the pressure record indicated a radius for R of about 7 km when fitted to a Holland (1980) profile and the storm centre was estimated as being 7 km from the site at the time of the peak measured

gust (Bureau of Meteorology 1977).

This geometric assessment suggests that the Dines may well have measured the peak gust at this site before it failed.

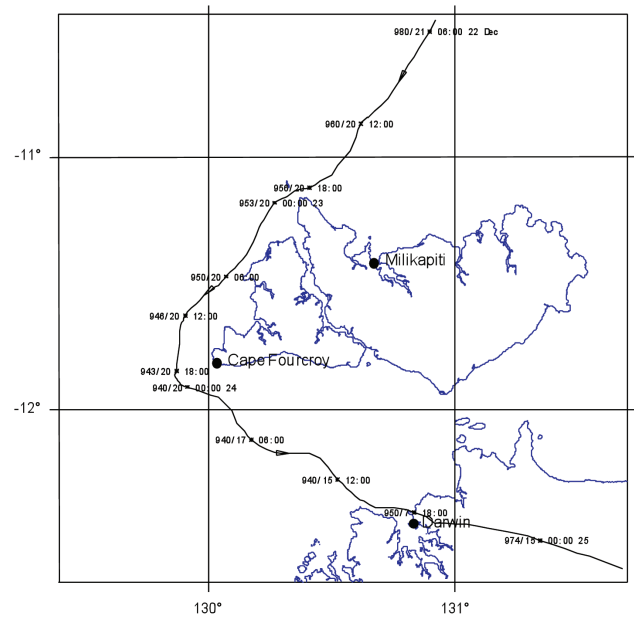
Reconstruction of the wind and pressure field

The reconstruction proceeded by commencing with the slightly modified intensity time series available from a review of historical tropical cyclones in the region (Harper et al. 2008), which placed it at its nominal peak intensity of 950 hPa when off Cape Fourcroy at 1130 UTC on 23 December. This level of intensity is assigned more than a day earlier than the National Climate Centre official track intensity details. The storm track was then augmented by blending the coarse 0.1° official fixes with the very detailed radar track given in Bureau of Meteorology (1977), including the observed trochoidal motion of the centre. The radar data previously used to estimate the diameter of the ‘inner eye’ of the storm was also collated and some estimates of an apparent ‘outer eye’ diameter were added based on the published sequence of radar images, which suggest an eyewall replacement cycle may have occurred. The latter could only be done approximately due to the small size of the images, but these scale estimates provide valuable guidance on the spatial changes taking place, especially as the centre neared the Cox Peninsula.

It is unfortunate that there was very little synoptic data in the area at this time. The only officially reporting station near the storm as it approached was Snake Bay (Milikapiti) located on the north coast of Melville Island, some 110 km NNW of Darwin and no closer than 45 km from the centre. One important observation at Cape Fourcroy is plotted on Fig. 12 in Bureau of Meteorology (1977), indicating 65 knots at 2030 UTC on 23 December with the centre within 14 km. By comparing the Milikapiti data with the Cape Fourcroy estimate and accounting for position and radar size, it was found necessary to specify a more intense central pressure at the time of recurvature. A nominal 940 hPa at this time, combined with a radius to maximum winds R of 20 km and a Holland B of 2.4 yielded a consistent model comparison between these sites. A simplistic assumption was then devised of a shrinking storm that weakened shortly before reaching Darwin to match the observed size and intensity at landfall, namely an R of 7.5 km and central pressure p_c of 950 hPa. Although not a conventional concept (shrinking and weakening), this construct provided close matching with the airport anemometer while assuming a constant B value of 2.4. The final track is presented in Fig. 4 together with indicated central pressure and adopted radius to maximum winds, while Fig. 11 shows further detail of the passage over Darwin.

Initial storm surge modelling proceeded at this point on the assumption that the storm parameters were sufficiently known to enable a reasonable reconstruction of the storm tide event. Unfortunately this was not the case and the modelled storm surge was significantly lower than recorded

Fig. 4 Reconstructed track of tropical cyclone *Tracy*.



(refer following section). After many trials, it became clear that the storm would have had to have maintained its (adjusted) maximum intensity (say 940 hPa) and its size (say 20 km) almost to the point of landfall in order to generate a storm surge of the magnitude required. However, this specification would lead to a very significant overestimation of the winds at Darwin airport during the twelve hours prior to landfall, which were very weak at around 5 to 7 ms⁻¹. While atmospheric stability may have played a part in suppressing vertical mixing, it seemed possible that the storm may have undergone significant ‘steepening’ of its wind profile in concert with the observed shrinking of the outer circulation after it turned almost on the coast near the Cox Peninsula and moved slowly eastwards.

During the approach to land at Darwin, it was determined that the radius to gales of the system would need to have been about 25 km in order to not overpredict the measured winds at the airport and to simultaneously generate the observed storm tide. More commentary on the storm tide aspect is included later.

Details of the modified Holland wind model are provided in Harper (2001) but it is important to note the gradient to surface boundary layer assumption in the adopted formulation, which affects the choice of the B parameter via:

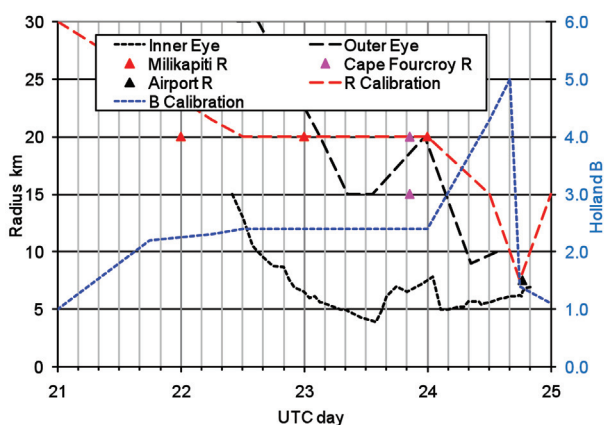
$$V_{\max} = K_m V_{g\max} = K_m \sqrt{\frac{B(p_n - p_c)}{\rho e}} \quad (1)$$

where V_{max} = maximum surface (+10 m) mean wind speed (ms^{-1})
 V_{gmax} = gradient level wind speed (ms^{-1})
 K_m = boundary layer factor
 p_n = ambient (outer open isobar) MSL pressure (Pa)
 p_c = central MSL pressure (Pa)
 B = Holland windfield peakedness parameter
 ρ = air density (kg m^{-3})
 e = exponential constant

The model adopted here assumes a nearly-constant factor K_m of 0.67, which has been developed and verified over many years in numerous storm surge and wave modelling contexts (e.g. Harper 2001, Harper et al. 2001). Based on more recent research (e.g. Kepert and Wang 2001) it is now generally accepted that while this value is reasonably representative of the outer windfield on the left-hand side (southern hemisphere) of a moving tropical cyclone (i.e. the stronger side due to forward motion), it presents as a complex radial and azimuthal pattern that is a function of many other variables. For example, on the right-hand side, K_m values are likely higher and towards the eyewall can approach or exceed 1.0, albeit in a very narrow zone. Accordingly, a higher K_m will allow a lower B to produce the equivalent surface wind speed, although as noted by Willoughby and Rahn (2004), the Holland profile shape at the eyewall is much broader than measured by aircraft. Hence, the adopted K_m and enhanced B combination here likely acts to better represent this extremely small storm. In any case, it must be acknowledged that this is a very simple model of a complex process, which is justified here by comparison with the observed independent data (wind, pressure, surge and wave action), and that other parameter combinations remain possible.

In summary, the calibrated storm R and B parameters are shown in Fig. 5, together with trends from the radar

Fig. 5 Summary of the calibrated R and B parameters for Tracy.



data and the fitting to regional observations as previously mentioned. The key to the calibration process has been the assumption of shrinkage and steepening of the wind and pressure profile during the 24 December approach into Darwin. The (nominal) B value of five required to achieve this is acknowledged as being far outside the normally accepted range of 1 to 2.5 (Holland 1980), which is based on inertial stability considerations. However, as discussed above, it is the present K_m and B combination that acts to provide the necessary profile steepness. For example, a K_m of 0.9 would match the airport wind peak with a B of 1.3, but the profile would be far too broad. It can be shown that the prescribed increase in B here is also less than might be justified based solely on conservation of angular momentum. It seems possible therefore that frictionally forced convergence during the period of prolonged near-coast interaction caused the 'outer eye' to rapidly converge onto the 'inner eye', which had been clearly seen on radar for several days. This apparent eyewall replacement cycle is summarised on Fig. 5 and better follows the conventional 'shrinking and intensifying' process, but culminating in a final weakening event at landfall that is probably more related to some type of inner eye instability than a new outer eye being established.

A large number of parameter trials were conducted to arrive at this combination, including consideration of 'double Holland' radial wind and pressure profiles (e.g. Thompson and Cardone 1996) to try to capture an inner and outer structure variability more sympathetic to the inferred radar patterns. Unfortunately the number of degrees of parameter freedom far exceeded the number of independent data points to sufficiently inform the fitting process. The result of that exercise was ultimately found not to be superior to the simpler single vortex model, possibly due to the extremely small scale of the overall storm.

In support of the above, Fig. 6 presents the comparison of modelled and measured¹ wind and pressure at the Darwin sites. Compared with the airport Dines, the modelled winds show a slightly broader peak and are slightly higher but otherwise are a very good match. As mentioned previously, a slightly better fit can be obtained without the assumed dynamic changes over the preceding 12 hours but only the present combination comes close to explaining all the observed features (see Fig. 8). The pressure comparison is given both at the WSO and at the RO, where the model can be seen to be discriminating the 6 km spatial offset reasonably well. In both cases however, the model has a steeper approach shape than measured. After eye passage, the manual adjustments have been successful in matching the apparently rapid decay and expansion of the eye. Fig. 7

¹The measured peak gust winds have been manually digitised from the hardcopy Dines record as the National Climate Centre electronic record is not sufficiently detailed. The measured mean wind, which is difficult to objectively estimate from the chart record, was then based on a 10-min to 3-s gust factor of 1.41, the commonly used assumption by meteorologists. The same assumption is then made in the modelling but in the reverse manner. Accordingly, the 1.41 factor here has been prescribed, although it is not an unreasonable value based on the observations.

Fig. 6 Comparison of measured and modelled winds and pressure at Darwin.

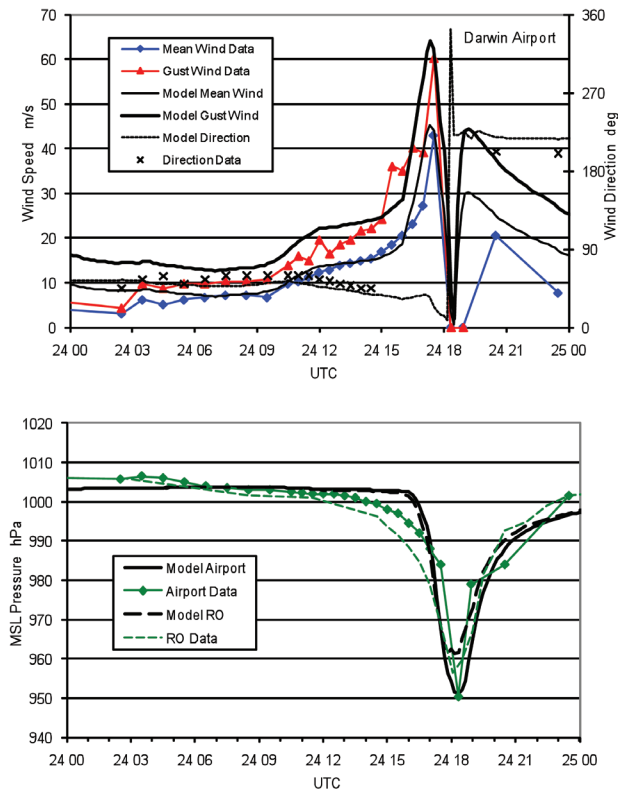
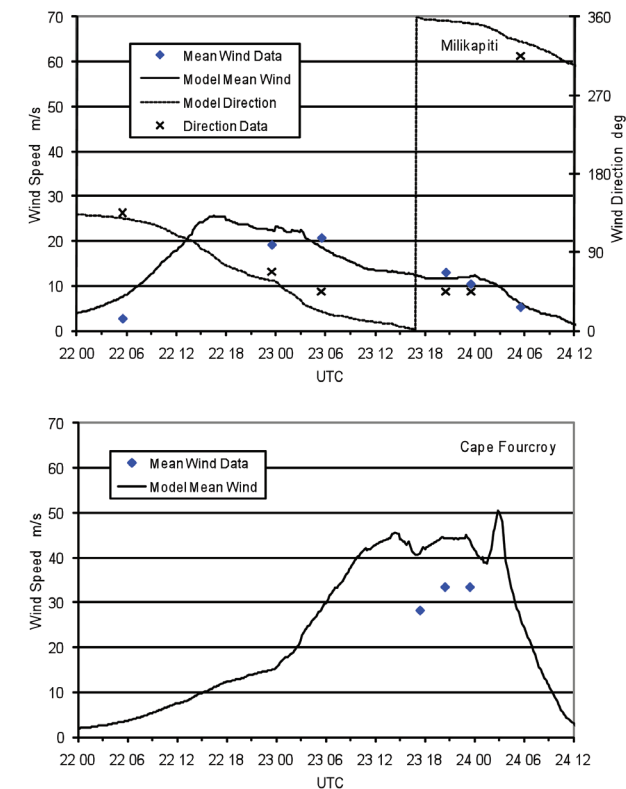


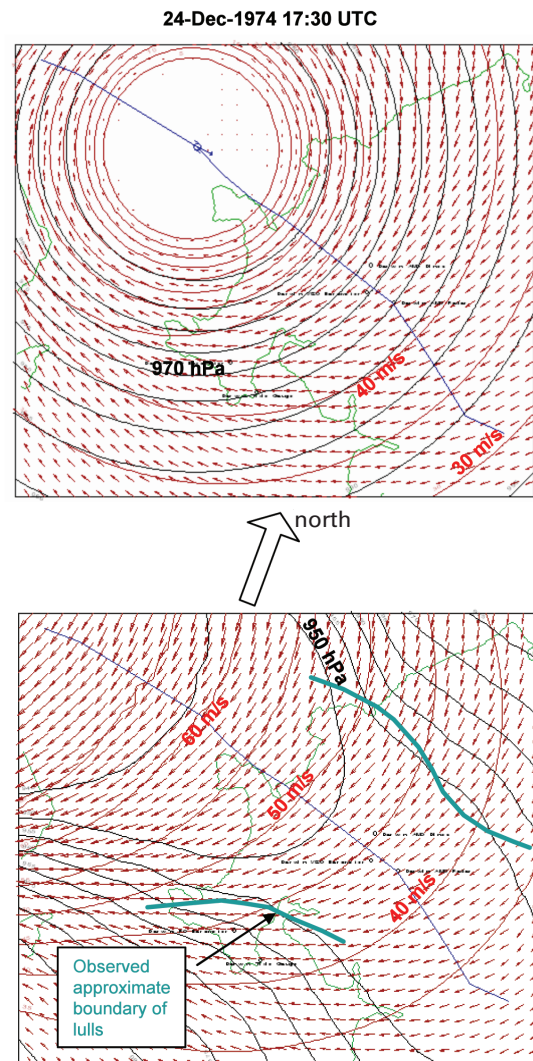
Fig. 7 Comparison of measured and modelled winds and pressure at Milikapiti and Cape Fourcroy.



presents the comparisons at Milikapiti and Cape Fourcroy. The model does a reasonably good job of matching the rather sparse data available from Milikapiti but significantly overpredicts Cape Fourcroy winds².

In support of the relatively dynamic parameter changes made, Fig. 8 shows the modelled spatial wind and pressure field at the time of the maximum recorded winds at the airport. The time snapshot in the top panel shows the storm centre just offshore, vectors of mean wind and contours of wind speed in 5 ms^{-1} intervals (red) and contours of MSL pressure on 5 hPa intervals (black). The bottom panel is the peak envelope (or swath) of the mean wind and MSL pressure. Overlaid on the swath is the Bureau of Meteorology

Fig. 8 Reconstructed mean wind and pressure field of tropical cyclone Tracy at landfall.



²No specific commentary on conditions at Cape Fourcroy was found in BoM (1977) although two sets of observations are reported on p5. In the analysis here, the observation was originally incorrectly interpreted as 100 kn but was later confirmed as 65 kn by G. Crane (BoM, pers. comm.). Unfortunately it was not possible to re-perform the extensive calibrations in the present study context to improve the comparisons at this location, but the impact on the overall conclusions is deemed relatively small.

(1977) estimate of the boundary of the lull based on personal reports and this can be seen to be in good agreement with the pressure pattern, showing both a decrease in intensity and a narrowing of the eye during this time. This type of detailed pattern could not be obtained without the dynamic assumptions discussed previously and is offered as further support for this phenomenon.

One interesting conclusion from Fig. 8 is that some of the suburbs seaward of the airport that were devastated may well have experienced mean winds of more than 50 ms^{-1} or gusts in excess of 70 ms^{-1} , but still be consistent with the Dines recording at the airport. Finally, Fig. 9 shows the full swath of modelled mean wind and pressure for the lifetime of *Tracy*, illustrating the speculated dramatic shrinking process as it approached Darwin. The inner-most swath wind speed contour (red) is 65 ms^{-1} with interval of 5 ms^{-1} , inner-most MSL pressure is 940 hPa (black) with interval of 5 hPa and the storm track is in blue. Maximum wind speed vectors are shown based on a resolution of 10 km. Coastline is in green.

Hydrodynamic modelling

A series of three nested computational domains were established representing the coastal features and the depths of the surrounding seas (Fig. 10). A spherical coordinate system was utilised for hydrodynamic modelling, while a flat Cartesian system was utilised for spectral wave modelling.

Almost the entire region's coastline is devoid of detailed land elevation data. Accordingly, for the A and B domains, the coastline is modelled as a 'vertical wall' at the location of the Mean Sea level (MSL) contour. For large-scale modelling in the absence of detailed survey data, the 'vertical wall' assumption is reasonable and will generally result in slightly over-estimated storm tide levels at the MSL contour in areas where there are immediately adjacent low lying regions. For the fine-scale C domain, overland flooding above MSL is permitted by the specification of land heights up to an elevation of +10 m, although only the immediate Darwin region has been accurately mapped. Details of each model domain are summarised below in Table 1.

The hydrodynamic model domains were constructed by the James Cook University Marine Modelling Unit (MMU)

Fig. 9 Reconstructed lifetime swath of wind and pressure fields for tropical cyclone *Tracy*.

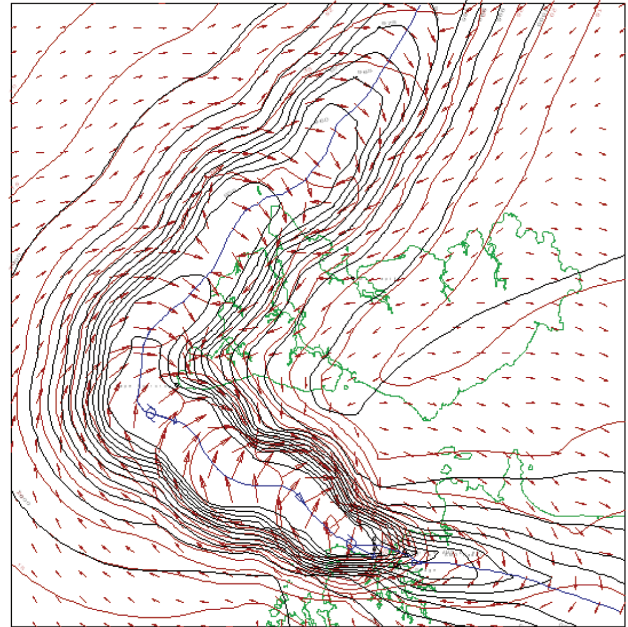
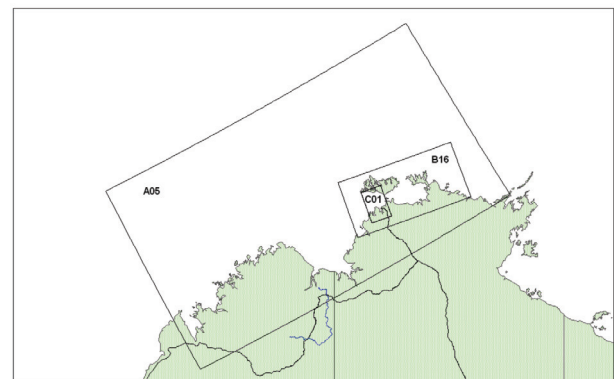


Fig. 10 The nested numerical hydrodynamic model domains.



and were produced using in-house MMU software that interpolates the available data onto the required grids. The software accepts non-uniform data in triples containing longitude, latitude and depth. Bathymetry data has been sourced mainly from digitised navigational charts (both Royal

Table 1. Numerical modelling domains.

Domain	Grid Origin		Grid Angle	Grid Size		Spatial Resolution		Spatial Extent	
	Lat	Lon	X axis bearing	X	Y	deg	km	km	km
	deg	deg	deg	Along Shore	Off Shore				
A05	-18.65	123.76	60	109	63	0.125	13.90	1501	862
B16	-13.57	129.92	70	185	91	0.025	2.78	511	250
C01	-13.00	130.47	70	161	251	0.005	0.56	89	139

by up to 1 to 2 h. When combined with the tide, the matching was almost exact, although the model still predicted slightly more drawdown in levels over the preceding day and missed some small oscillations immediately following the peak surge. After making the various storm parameter modifications, the results of the surge modelling combined with the tide are graphed in the top panel of Fig. 12 as the solid red line, which shows the excellent matching with the tide gauge levels. In the lower graph is the comparison of the measured and modelled residual (surge). Also shown is the 'initial modelled' result prior to the storm modifications, where the modelled surge was only 0.75 m (dashed red line).

The resulting pattern of storm surge development near Darwin is summarised in the two panels of Fig. 13, which show the model prediction at 2 h before the time of the peak tide gauge height and at the time of the peak. The panels show the water velocity pattern and the contours of surge level in 0.5 m intervals relative to MSL. The green regions are land above 10 m MSL, while the plain white areas are potentially subject to wetting and drying during the simulation. The storm track and position of the storm centre is overlain on each panel, together with sites of interest. The top panel is at the time of the radar image in Fig. 2 and shows the storm surge developed along the coast from Cape Charles east to Waugait. In the bottom panel 2 h later, the storm centre

is opposite the harbour entrance and has driven the surge well into the harbour, where levels are just below 1.5 m at this time in most areas. The circle of maximum winds has a radius of about 8.5 km and can be seen to be driving large currents onto the coast in its vicinity.

Numerical modelling of waves and wave setup

Unfortunately there were no measurements of wave heights available anywhere in the Darwin area during the storm passage. Only unsurveyed beach debris estimates were available of the combined effects of the storm tide and wave runup on the open bay beaches.

The ADFA1 2nd generation spectral wave model (Young 1988) was used for wave modelling throughout the region. Analogous views to the preceding storm surge patterns are presented in Fig. 14 that show the predicted wave height patterns. The spectral wave modelling was originally undertaken at a fixed MSL depth as the changes in water level close to the coast were thought unlikely to significantly influence the shoaling and refraction processes. The model results are presented with a significant wave height contour interval of 1.0 m and the length of the directional vectors is proportional to the wave period. In the wave model, the wetting and drying is not relevant and so all land above MSL is indicated. The first panel shows the region of highest

Fig. 13 Modelled surge pattern relative to MSL during *Tracy*.

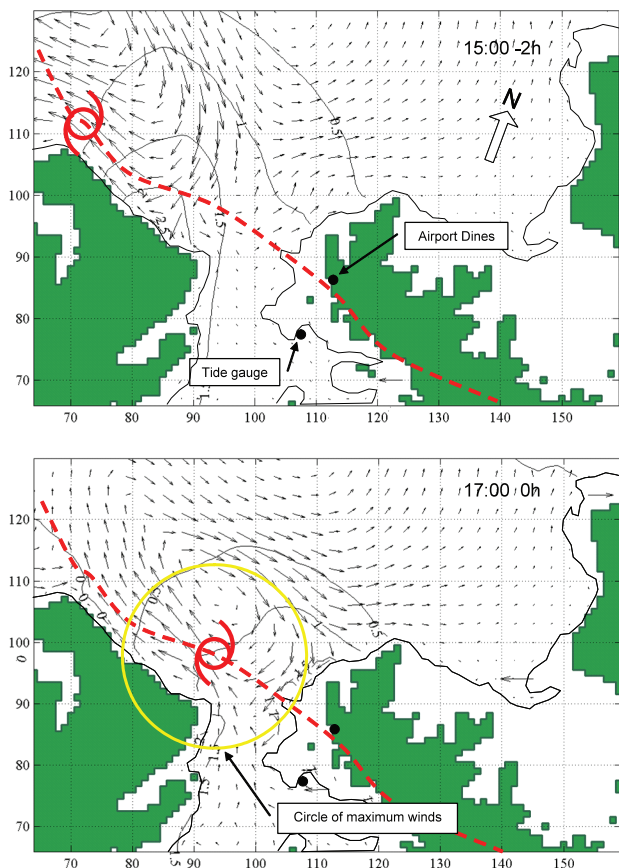
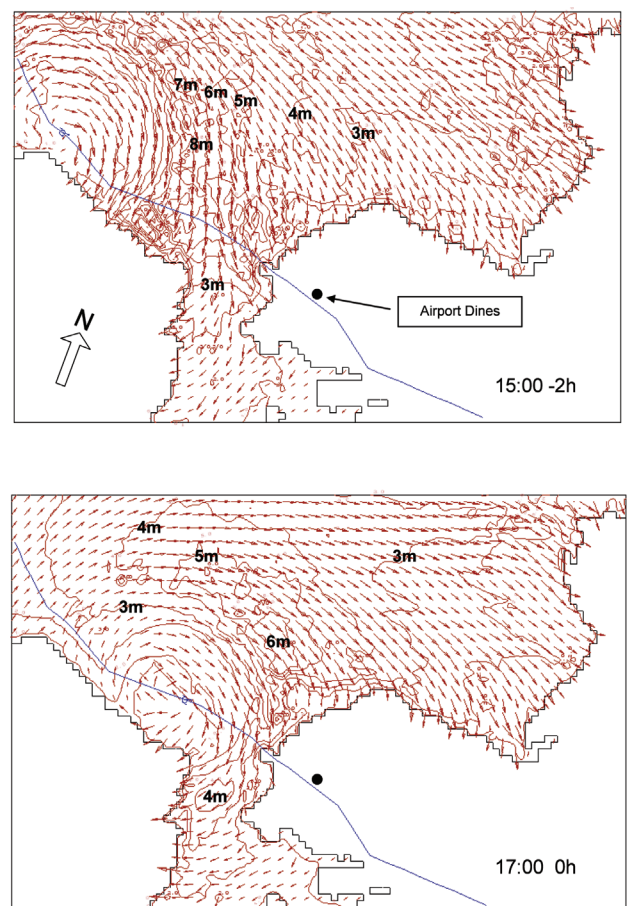


Fig. 14 Modelled storm waves during Cyclone *Tracy*.



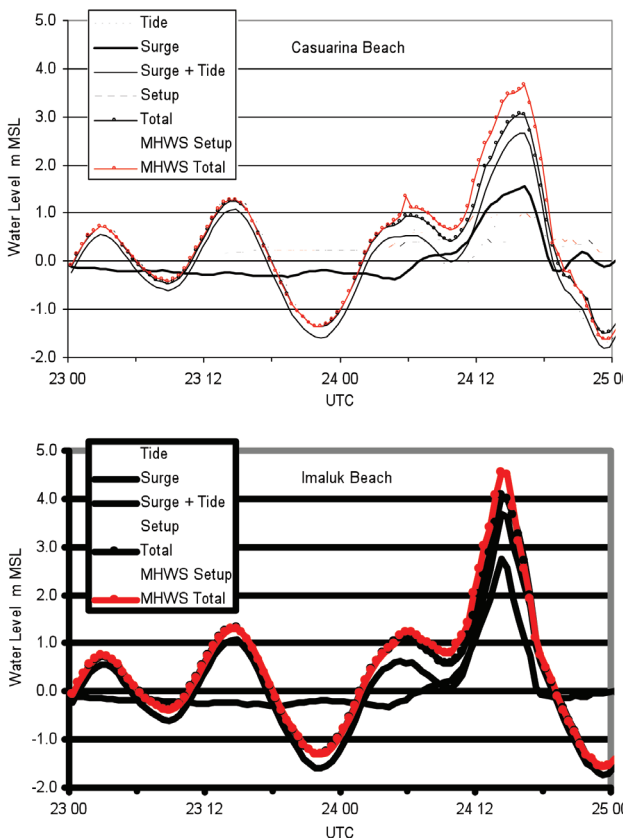
significant waves (8 m) at this time is north of the harbour entrance. In the bottom panel this region of highest waves has impacted the coast and undergone significant breaking, while waves up to 4 m have propagated into the harbour entrance. It is the open coast east of Nightcliff that receives the full impact of the incoming waves and it is there that wave setup and runup effects could be expected to have been greatest.

Total storm tide estimates during Tracy

The modelled nearshore wave height and period information was then converted into a vertical wave setup estimate at the shoreline using the analytical approach after Hanslow and Nielsen (1993), which is based on radiation stress concepts calibrated against field measurements on sandy beaches. The resulting time history of total storm tide was then obtained by linearly adding the predicted MSL-referenced tide, storm surge and setup time histories for sites of interest. This is illustrated in Fig. 15, for the case of Casuarina Beach, which experiences the highest predicted levels near Darwin, and also for Imaluk Beach 20 km to the west on the opposite side of the harbour, which has the highest predicted levels overall.

Both sites were estimated by the model to have experienced wave setup up of about 0.5 m. The top panel shows that the predicted Casuarina Beach peak level is

Fig. 15 Time histories of surge plus tide plus wave setup during Tracy.



about 3 m MSL, which compares with the absolute water level based on beach debris in Bureau of Meteorology (1977) of about 5 m (quoted as 4 m above tide). This additional increase could be due to localised wave runup (e.g. Harper et al. 2001). At Imaluk Beach, the model indicates a higher and sharper surge peak that results in a total storm tide level of 4 m based on the MSL assumption.

Subsequent review of the MSL fixed water level assumption lead to a decision to further examine the sensitivity of wave heights, and especially wave setup, to the assumed tide level. This was on the basis that premature wave breaking on the various offshore shoals might unduly prevent wave energy propagation onto nearby beaches. Accordingly, additional spectral wave modelling tests were conducted with a fixed tide level of MHWS (the model requires a fixed water level) which, at 2.8 m MSL, is close to the peak tide plus surge level experienced in the immediate region during Tracy. These are also shown in Fig. 15 and result in a near-doubling of the estimated wave setup components, bringing the modelled results closer to the debris estimates.

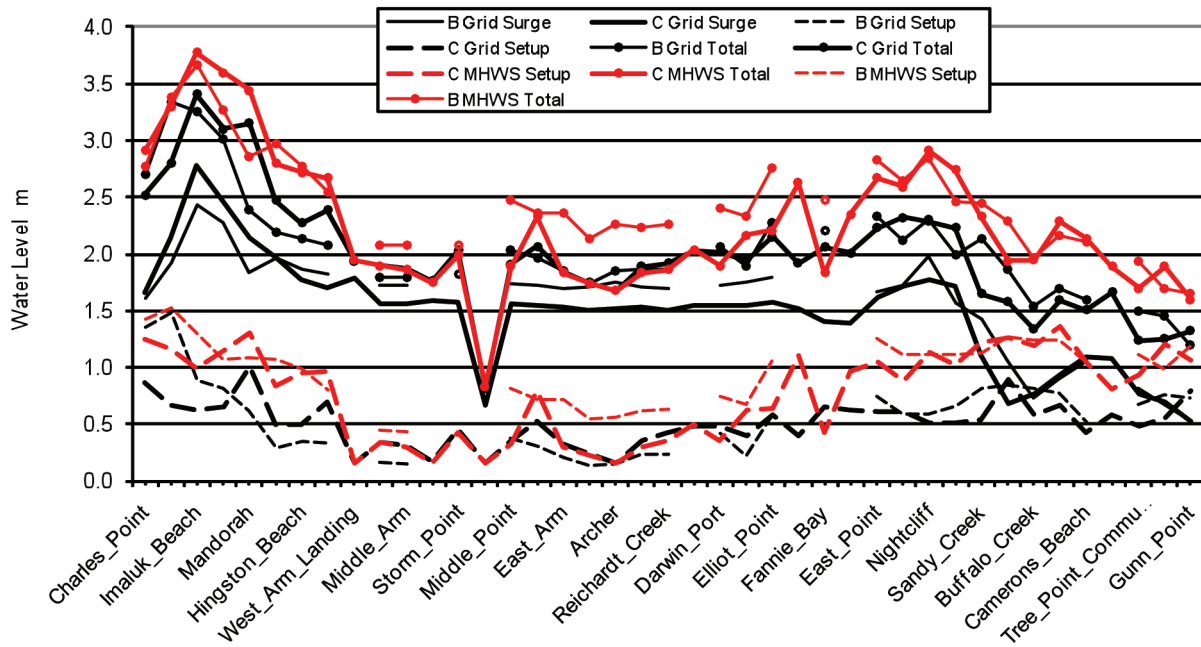
Fig. 16 provides a summary of the regional variation in surge, setup and total water level maxima (not dynamically coupled here) that extends from Charles Point to Gunn Point and also includes the coarse grid prediction (B). Here the Fannie Bay estimate compares well with the Bureau of Meteorology (1977) estimate of a 2 m surge.

Use of a fully coupled tide, surge and wave model plus radiation stress might modify the above conclusions slightly but significant departures from the uncoupled simulations are deemed unlikely. Importantly, more detailed bathymetry would also be required to support an increased sophistication in the wave analysis.

Conclusions

The accurate hindcasting of the Tracy storm surge required a careful consideration of the likely dynamical behaviour of the storm windfield as it neared Darwin. Initial attempts assuming a steady-state storm approach during 24 December well-matched the recorded winds and pressure at the Darwin Airport but failed to generate the measured peak surge of 1.55 m, reaching only 0.75 m. A large number of sensitivity tests using simplified analytical wind and pressure models were done to determine how the time history of both the wind and storm surge measurements could be simultaneously matched. As suggested by the series of radar images, it was speculated that the storm underwent significant structural change during the final period—likely an eyewall replacement cycle followed by vortex instability at landfall. After making various model parameter changes that affected the size, intensity and peakedness of the windfield, the storm surge and the wind and pressure records better matched available observations, and the modelled wind swath over Darwin also better matched eyewitness reports of the shrinking eyewall. As a result, it is speculated that the suburban areas between the

Fig. 16 Regional variability and effect of grid resolution when modelling Tracy.



airport and the coast, which were very extensively damaged, may have actually experienced higher wind gust speeds than measured by the Dines instrument – perhaps as high as 70 ms⁻¹.

Acknowledgments

This project, undertaken as part of the development of the Darwin Tropical Cyclone Warning Centre (TCWC) Northern Region Storm Tide Prediction System, and described in SEA (2005), was co-funded by an Emergency Management Australia Projects Program grant, a grant from the Northern Territory Emergency Service, and by the Disaster Mitigation program of the Australian Bureau of Meteorology.

Special thanks are due to Ross Christmas of the Northern Territory Regional Office for confirming accurate locations of the airport instrumentation and the R.O. at the time of Tracy.

References

- Bureau of Meteorology, 1977. *Report on cyclone Tracy December 1974*. Department of Science, Bureau of Meteorology, AGPS, Canberra.
- Cole E.K. 1977. *Winds of Fury*, Rigby.
- Hanslow D.J. and Nielsen P. 1993. Shoreline setup on natural beaches. *J. Coastal Res.*, Special Issue 15, 1-10.
- Harper B.A. (ed.), 2001. *Queensland climate change and community vulnerability to tropical cyclones - ocean hazards assessment - stage 1*, Report prep by Systems Engineering Australia Pty Ltd in association with James Cook University Marine Modelling Unit, Queensland Government, March, 375pp.
- [<http://www.longpaddock.qld.gov.au/AboutUs/Publications/byType/Reports/ClimateChange/VulnerabilityToTropicalCyclones/Stage1/Full-ReportLowRes.pdf> accessed 08/07/2010].
- Harper B.A. 2002. *Tropical cyclone parameter estimation in the Australian region: wind-pressure relationships and related issues for engineering planning and design – a discussion paper*. Prepared by Systems Engineering Australia Pty Ltd for Woodside Energy Ltd, Nov. [<http://www.uq.net.au/seng/download/>].
- Harper, B.A. and Holland, G.J. 1999. An updated parametric model of the tropical cyclone. *Proc. 23rd Conf. Hurricanes and Tropical Meteorology*, American Meteorological Society, Dallas, Texas, 10-15 Jan.
- Harper B.A., Hardy T.A., Mason L.B. and McConochie J.D. 2001. Cyclone Althea revisited. *Proc 15th Australasian conference on coastal and ocean engin.*, Coasts & Ports 2001, IEAust, Gold Coast, Sept.
- Harper B.A., Stroud S.A., McCormack M. and West S. 2008. A review of historical tropical cyclone intensity in north-western Australia and implications for climate change trend analysis. *Aust. Met. Mag.*, 57, 121-41.
- Holland G.J. 1980. An analytic model of the wind and pressure profiles in hurricanes. *Mon. Weath. Rev.*, 108, 1212-18.
- Keperth J. and Wang Y. 2001. The dynamics of boundary layer jets within the tropical cyclone core - Part II: nonlinear enhancement. *J. Atmos. Sci.*, 58, 2485-501.
- Mason L.B. and McConochie J.D. 2001. *MMUSURGE user's guide*. School of Engineering, Marine Modelling Unit, James Cook University, Townsville.
- SEA, 2005. *Darwin TCWC Northern region storm tide prediction system - system development technical report*. Prep by Systems Engineering Australia Pty Ltd for the Bureau of Meteorology, Darwin. SEA Report J0308-PR001C, 208pp, Dec.
- Thompson E.F. and Cardone V.J. 1996. Practical modelling of hurricane surface wind fields. *J. Waterways, Port, Coastal and Ocean Engineering*, ASCE, 122, 195-205.
- Walker G.R. 1975. *Report on Cyclone Tracy – effects on buildings – December 1974*, Australian Department of Housing & Construction, Melbourne, Vol. 1. (Available on <http://www.eng.jcu.edu.au/cts/learning.htm>).
- Willoughby H. E. and Rahn M.E. 2004. Parametric representation of the primary hurricane vortex. Part I: Observations and evaluation of the Holland (1980) model. *Mon. Wea. Rev.*, 132, 3033-48.
- Young I.R. 1988. A shallow water spectral wave model. *J. Geophys. Res.*, 93, 5113-29.

